JACS
JOURNAL OF THE AMERICAN CHEMICAL SOCIETY
Communication
pubs.acs.org/JACS

Luminescent Metal–Organic Framework Films As Highly Sensitive and Fast-Response Oxygen Sensors

Zhongshang Dou, Jiancan Yu, Yuanjing Cui,* Yu Yang, Zhiyu Wang, Deren Yang, and Guodong Qian*

State Key Laboratory of Silicon Materials, Cyrus Tang Center for Sensor Materials and Applications, Department of Materials Science and Engineering, Zhejiang University, Hangzhou, 310027, China

Supporting Information

ABSTRACT: Luminescent metal–organic framework films, CPM-5⊃Tb^{3+} and MIL-100(In)⊃Tb^{3+}, have been constructed by postfunctionalization of two porous indium–organic frameworks with different structures, respectively. The MIL-100(In)⊃Tb^{3+} film shows high oxygen sensitivity (K_{SV} = 7.59) and short response/recovery time (6 s/53 s).

Lanthanide metal–organic frameworks (MOFs) have emerged as very important multifunctional luminescent materials in the past decade due to their unique luminescence properties such as high luminescence quantum yield, long-lived emission, large Stokes shifts, and characteristically sharp line emissions.[1−4] The combination of these intrinsic luminescent features together with the inherent porosity of MOFs provides an effective platform for chemical sensing.[5] For practical sensor applications, it is of interest to fabricate MOFs as thin films on different types of substrates including Si or ITO glass to realize the optoelectronic integration circuits.[6,7] However, it is still a challenge to grow highly crystalline lanthanide MOF films on substrates due to the high coordination number and flexible coordination geometry of lanthanide ions. Fortunately, the incorporation of lanthanide ions within MOF films utilizing postsynthetic ion-exchange strategy should be expected to perform the similar luminescent sensing function of lanthanide MOFs. In fact, a number of guest species, such as lanthanide ions,[8,9] fluorescent dyes,[10] and quantum dots,[11,12] have been incorporated into bulk MOFs to create luminescence.

Up to now, tremendous luminescent complexes have been designed for oxygen sensing.[13,14] However, such materials are usually immobilized into porous polymeric or silica-based matrices,[15,16] resulting in severe losses on oxygen sensitivity due to the reduced surface area between interacted phases. Recently, a few porous MOF powders with high porosity and high luminescence from the organic ligands have been designed for oxygen sensing.[17−21] The characteristic luminescence of lanthanide MOFs can be ascribed to ligand-to-metal energy transfer (EnT), known as "luminescence sensitization" or "antenna effect".[1,2] Oxygen quenching of these MOFs is supposed to be resulted from the deactivation on triplet-state organic ligands by the oxygen molecule, which, on the other hand, has little interaction with the excited states of lanthanide ions, similar to that of lanthanide complexes.[14] Thus, for efficient oxygen sensing, the energy transfer processes of lanthanide-centered MOFs should contain not only an effective EnT but also an appropriate thermally activated energy back transfer (BEnT) to prolong the triplet-state lifetime of ligands.[22,23] As a result, it is expected that differences in energy transfer rates of MOFs may lead to significant variations in oxygen sensing capabilities. In this concern, it is suggested that the introduction of Tb^{3+} into two indium trimesate MOFs, $[(CH_3)_2NH_2][In_3O(BTC)_2(H_2O)_3]_2[In_3(BTC)_4]$ (denoted as CPM-5)[24] and $In_3O(OH)(H_2O)_2[BTC]_2$ (denoted as MIL-100(In)),[25] in the presence or absence of extra carboxylate acid will make adjustment on energy transfer processes and thereby oxygen sensitivities possible. The first triplet-state energy of 1,3,5-benzenetricarboxylate (BTC) (23200 cm^{-1}, estimated from the phosphorescence peak at about 430 nm of $Gd(BTC)(H_2O)_6$ recorded at 77 K)[26] is close to the excited state of Tb^{3+} ($^5D_4$, 20400 cm^{-1}), resulting in effective EnT and appropriate BenT, which is beneficial to oxygen sensing (Scheme 1). Herein, we report two luminescent MOF films,

Scheme 1. Energy Transfer Processes and O_2 Quenching Processes of (a) CPM-5⊃Tb^{3+} and (b) MIL-100(In)⊃Tb^{3+}[a]

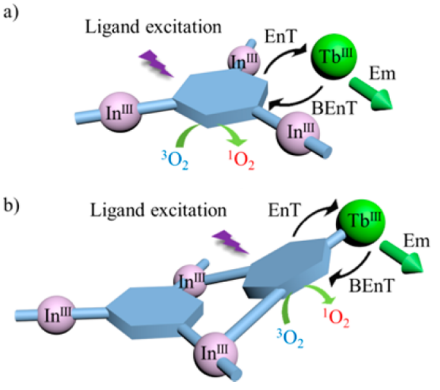

[a]EnT: energy transfer from the ligand to the metal ion. BEnT: energy back transfer. Em: emission.

CPM-5⊃Tb^{3+} and MIL-100(In)⊃Tb^{3+}, which are prepared via postfunctionalization of CPM-5 and MIL-100(In) with terbium ions, and their oxygen sensing capabilities are also demonstrated.

The CPM-5 and MIL-100(In) films were prepared by the in situ solvothermal synthesis method on ITO glass according to procedures reported previously.[27] Results of X-ray diffraction

Received: November 3, 2013
Published: April 3, 2014

   dx.doi.org/10.1021/ja411224j | J. Am. Chem. Soc. 2014, 136, 5527−5530

indicate that as-prepared films have structures the same as CPM-5 and MIL-100(Al), respectively (Figure S1 in the Supporting Information). CPM-5 possesses a large guest-accessible volume (47.9% of the total volume) with pore size of 4.89 Å, and MIL-100(In) has pores with free inner diameters of about 20 and 26 Å, which are desirable for postmodification and oxygen sensing.[24,25] In CPM-5, all carboxylate acids of H_3BTC ligand are deprotonated and $(CH_3)_2NH_2^+$ serves as the movable charge-balancing cation in pores. In MIL-100(In), it is expected that there might be extra trimesic acid which has strong interaction with the In_3O trimer through the CO−In monodendate coordination and serves as one of the terminal molecules of the In_3O trimer, which also occurs in MIL-100(Al).[28−31] The morphology of the CPM-5 and MIL-100(In) films is studied by scanning electron microscopy (SEM) (Figure S2 in the Supporting Information). The MOF crystals pack tightly to each other, and good adhesion between the continuous MOF layers and the ITO surface is seen. The MOF films do not break off from the substrates after the ultrasonic washing in the water or ethanol for 30 min. Based on our previous studies,[22] the indium(III) oxide on the substrate is essential to the growth of continuous films, which can improve the homogeneous nucleation and growth. Sufficient nucleation precursors on substrate surfaces are provided by the two indium sources in the solution and on the ITO glass during the formation of small MOF crystals. The CPM-5 and MIL-100(In) films prepared in the solvothermal solutions with 12.5 mmol·L^{-1} of $In(NO_3)_3$ or $InCl_3$ and 12.5 mmol·L^{-1} of H_3BTC have the same thickness of about 2.5 μm. It should be noted that the film thickness can also be adjusted easily by varying the reactant concentration (Figures S3 and S4 in the Supporting Information).

Luminescent CPM-5⊃Tb^{3+} and MIL-100(In)⊃Tb^{3+} films are prepared by immersing indium−organic framework films in 3 mL DMF solutions with 0.2 mol·L^{-1} of $Tb(NO_3)_3·6H_2O$. The X-ray diffraction patterns (Figure S1 in the Supporting Information) and SEM images (Figure 1) of CPM-5⊃Tb^{3+} and MIL-100(In)⊃Tb^{3+} films confirm that the modifications of indium−organic frameworks barely change the structures and the morphology of the MOF films. The Tb 4d XPS core level spectra were recorded to study the chemical state of terbium ion in CPM-5⊃Tb^{3+} and MIL-100(In)⊃Tb^{3+} films (Figure S5 in the Supporting Information). The Tb 4d peak of CPM-5⊃Tb^{3+} is close to the peak of $Tb(NO_3)_3$, indicating that the terbium ions of CPM-5⊃Tb^{3+} and $Tb(NO_3)_3$ have similar binding energy and electron density. It is suggested that the terbium ion in CPM-5⊃Tb^{3+} serves as the charge-balancing Tb^{3+} in the pores, which is commonly observed on other lanthanide ions, cationic chromophores, and metal ions in anionic MOFs.[8,10,32] The Tb 4d XPS spectrum of MIL-100(In)⊃Tb^{3+} is similar to that of $Tb(NO_3)_3$. However, its peak position at 151.4 eV is lower by about 1.2 eV than that of $Tb(NO_3)_3$ at 152.6 eV, which can be ascribed to the coordinate covalent bond of Tb−O between Tb^{3+} and carboxylate acid in the MOFs, leading to an increase in the electron density of terbium ion while a decrease in the binding energy.[33] The coordination environments of Tb^{3+} in both Tb@CPM-5 and Tb@MIL-100(In) are further confirmed by X-ray absorption fine structure (XAFS, Figure S6 in the Supporting Information), and the possible schematic illustration of terbium ions in the MOFs is presented in Figure S7 in the Supporting Information.

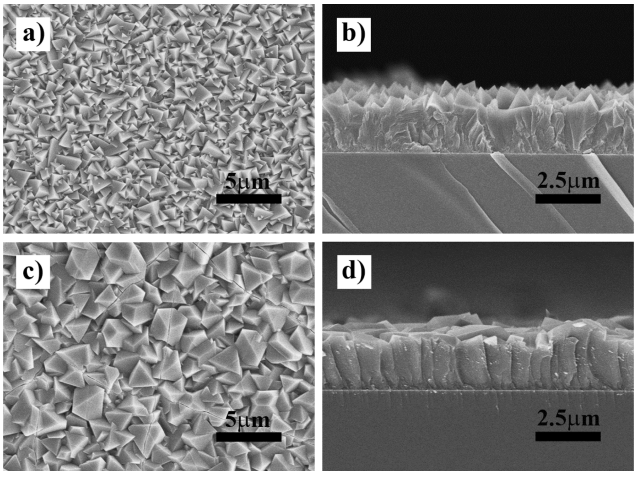

Figure 1. SEM images of CPM-5⊃Tb^{3+} (a, b) and MIL-100(In)⊃Tb^{3+} (c, d) films.

The luminescent properties of postfunctionalized MOF films were studied (Figure S8 in the Supporting Information). Broad excitation bands peaking at 285 nm are observed in the excitation spectra of CPM-5⊃Tb^{3+} (λ_{em} = 544 nm) and MIL-100(In)⊃Tb^{3+} (λ_{em} = 546 nm), indicating the presence of energy transfer from the BTC ligand to Tb^{3+}. Both the characteristic emission bands of Tb^{3+} and the emission of the BTC ligand peaking at 368 nm are found in the luminescence spectrum of the as-prepared CPM-5⊃Tb^{3+} film, suggesting relatively low energy transfer efficiency from the BTC ligand to Tb^{3+}. For the MIL-100(In)⊃Tb^{3+} film, the emission of Tb^{3+} becomes much more prominent while the emission of the BTC ligand can be ignored. The luminescence lifetime and quantum yields of CPM-5⊃Tb^{3+} and MIL-100(In)⊃Tb^{3+} were also measured (Table S3 in the Supporting Information). The quantum yield of MIL-100(In)⊃Tb^{3+} film is about 16.8%, much higher than that of CPM-5⊃Tb^{3+} (1.1%). The much higher energy transfer efficiency of MIL-100(In)⊃Tb^{3+} in comparison with that of CPM-5⊃Tb^{3+} is in good accordance with the presence status of terbium ions in two MOFs. The Tb^{3+} in MIL-100(In)⊃Tb^{3+} is sensitized by the intramolecular energy transfer process while that in CPM-5⊃Tb^{3+} is sensitized intermolecularly. Thus, the higher energy transfer efficiency of MIL-100(In)⊃Tb^{3+} can be ascribed to its shorter donor−acceptor distance, according to Dexter's exchange mechanism.[34]

To demonstrate the feasibility for oxygen sensing, emission spectra of activated CPM-5⊃Tb^{3+} and MIL-100(In)⊃Tb^{3+} films with the thickness of about 2.5 μm (as shown in Figure 1) were in situ recorded under oxygen gases with defined oxygen partial pressure Po_2 in nitrogen, 0, 1/6, 1/3, 1/2, 2/3, 5/6, and 1 atm (Figure 2). The emission intensities of activated films decrease gradually with the increase in Po_2. Because of the small energy gap between the first triplet state of BTC and the $^5D_4$ of Tb^{3+}, thermally activated back energy transfer from the $^5D_4$ energy level of Tb^{3+} to the triplet state of BTC occurs at ambient temperature, leading to the establishment of a photoequilibrium which extends the triplet-state lifetime of the BTC.[14,35] When the oxygen molecule diffuses into the MOF pores, the triplet state of BTC may be deactivated subsequently by the triplet oxygen via bimolecular collisions,[15] resulting in the gradually quenched luminescence of activated films with the increasing Po_2. At 1 atm of O_2, the quenching

dx.doi.org/10.1021/ja411224j | J. Am. Chem. Soc. 2014, 136, 5527−5530

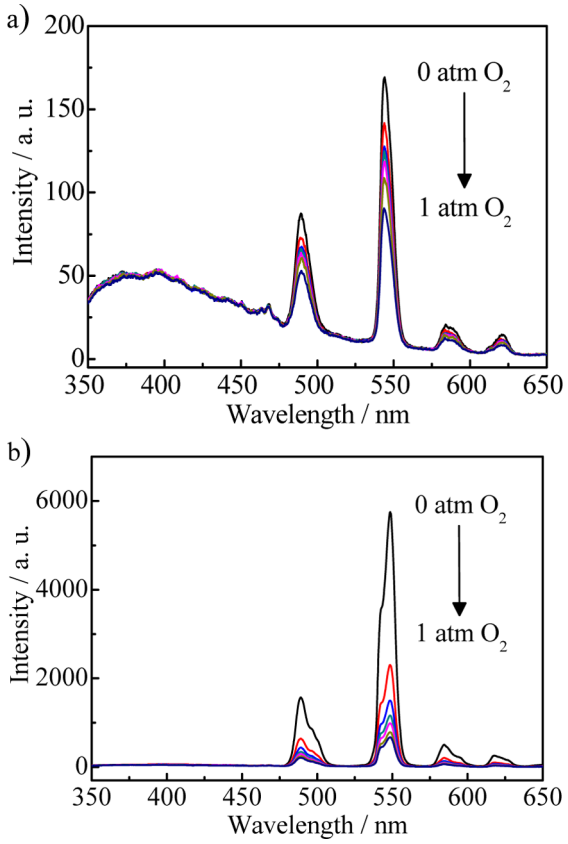

Figure 2. Emission spectra of activated (a) CPM-5⊃Tb^{3+} and (b) MIL-100(In)⊃Tb^{3+} films under different oxygen partial pressure Po_2.

efficiencies of activated CPM-5⊃Tb^{3+} and MIL-100(In)⊃Tb^{3+} films are about 47% and 88%, respectively. Thus, luminescent sensing capabilities of oxygen gas are expected for these two MOF films.

Oxygen quenching is diffusion-limited and can be described by the linear Stern−Volmer relation in homogeneous microenvironment materials.[15,31,32] Good linearity can be seen from the Stern−Volmer plots (I_0/I vs Po_2) of the activated CPM-5⊃Tb^{3+} and MIL-100(In)⊃Tb^{3+} films prepared using 0.2 mol·L^{-1} $Tb(NO_3)_3{\cdot}6H_2O$ solution, as shown in Figure 3, suggesting that the Tb^{3+} within each MOF is distributed homogeneously. The oxygen sensing properties of the two films are summarized

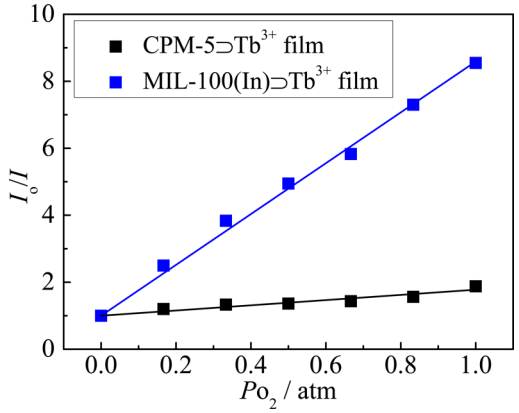

Figure 3. Stern−Volmer plots showing I_0/I vs oxygen partial pressure Po_2 for the activated MOF films.

in Table S4 in the Supporting Information. The Stern−Volmer quenching constant K_{SV} of CPM-5⊃Tb^{3+} and MIL-100(In)⊃Tb^{3+} films are estimated to be 0.78 and 7.59 respectively. For CPM-5⊃Tb^{3+} and MIL-100(In)⊃Tb^{3+} films, the I_0/I_{100} values are larger than the reported Yb^{3+}-incorporated MOFs.[8] The MIL-100(In)⊃Tb^{3+} film shows promising *Ksv* or I_0/I_{100} values that are much larger than those of many other MOF powders based on the phosphorescence of organic ligand.[17−20] The sensitivity of MIL-100(In)⊃Tb^{3+} film is also larger than the polymeric matrixes doped with Eu complexes.[35] It is exhibited that the oxygen sensitivity of the activated MIL-100(In)⊃Tb^{3+} film is almost 1 order magnitude higher than that of the CPM-5⊃Tb^{3+} counterpart. It can be pronounced that luminescent lanthanide-centered MOFs with intramolecular energy transfer exhibit higher oxygen sensitivities than the MOFs with intermolecular energy transfer when the lanthanide ions are sensitized by the same organic ligand. Also, the detection limits for CPM-5⊃Tb^{3+} and MIL-100(In)⊃Tb^{3+} films are about 1.7% and 0.4%, respectively.

The luminescence intensities of activated MOF films within alternating cycles of 1 atm of O_2 and 1 atm of N_2 indicate that activated MOF films have reversible oxygen quenching and nitrogen recovering properties (Figure 4). At the excitation

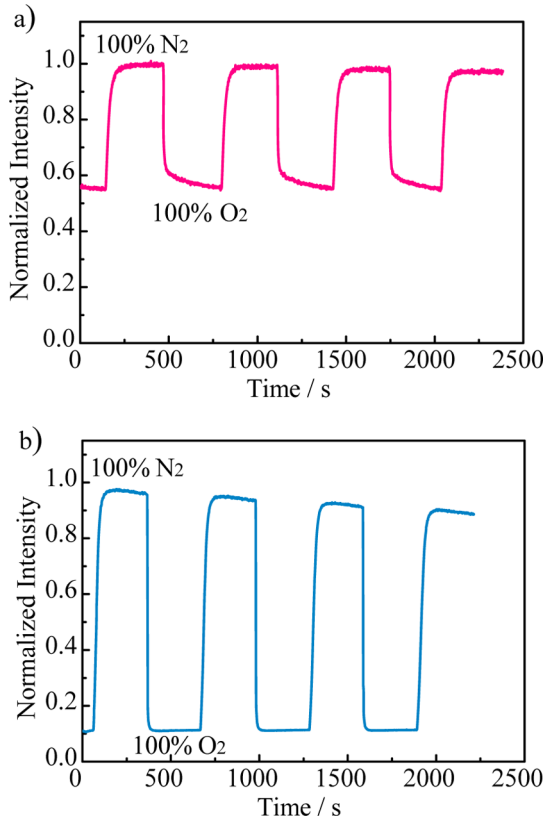

Figure 4. Reversible luminescence quenching of (a) CPM-5⊃Tb^{3+} film and (b) MIL-100(In)⊃Tb^{3+} film upon alternating exposure to 1 atm of O_2 and N_2.

wavelength of 285 nm, emission intensities of CPM-5⊃Tb^{3+} and MIL-100(In)⊃Tb^{3+} films at 544 and 548 nm respectively are monitored with the elapse of time. Because of the high porosity of MOFs, the diffusion of oxygen is fast in the MOF films. In the case of the CPM-5⊃Tb^{3+} films, it takes about 90 and 60 s respectively to accomplish 95% of the overall

dx.doi.org/10.1021/ja411224j | J. Am. Chem. Soc. 2014, 136, 5527−5530

luminescent intensity variation from 100% N_2 to 100% O_2 and vice versa, while in the case of the MIL-100(In)⊃Tb^{3+} films, it takes only about 6 and 53 s respectively under the same experimental conditions. The short response and recovery time of MOF films toward oxygen allows for reversible and rapid detection of O_2 molecules.

In summary, two luminescent MOF films based on Tb^{3+} have been constructed by postfunctionalization of indium−organic framework films, CPM-5 and MIL-100(In). The luminescent MOF films with high porosity exhibit fast and reversible detection of oxygen. The energy transfer efficiency of MIL-100(In)⊃Tb^{3+} is much higher via the binding interaction between the extra carboxylate acid and incorporated terbium ion in MOF pores than that of CPM-5⊃Tb^{3+} in which the terbium ion serves as the mobile charge-balancing cation. The MIL-100(In)⊃Tb^{3+} film shows higher oxygen sensitivity (K_{SV} = 7.59) and shorter response/recovery time (6 and 53 s) than those of CPM-5⊃Tb^{3+} film. It is believed that the porous luminescent MOF films will provide great potential in applications for sensing gases or vapors with high sensitivity.

■ ASSOCIATED CONTENT

Supporting Information

Experimental procedures and characterization data. This material is available free of charge via the Internet at http://pubs.acs.org.

■ AUTHOR INFORMATION

Corresponding Authors

cuiyj@zju.edu.cn
gdqian@zju.edu.cn

Notes

The authors declare no competing financial interest.

■ ACKNOWLEDGMENTS

This work was supported by the National Natural Science Foundation of China (No. 51010002, 51272229, and 51272231) and Zhejiang Provincial Natural Science Foundation of China (No. LR13E020001). We thank beamline BL14W1 (Shanghai Synchrotron Radiation Facility) for providing the beam time. We also thank Prof. Y. F. Liu for assistance during the XAFS measurements.

■ REFERENCES

(1) Allendorf, M. D.; Bauer, C. A.; Bhakta, R. K.; Houk, R. J. T. *Chem. Soc. Rev.* **2009**, *38*, 1330−1352.
(2) Cui, Y.; Yue, Y.; Qian, G.; Chen, B. *Chem. Rev.* **2012**, *112*, 1126−1162.
(3) Cui, Y.; Xu, H.; Yue, Y.; Guo, Z.; Yu, J.; Chen, Z.; Gao, J.; Yang, Y.; Qian, G.; Chen, B. *J. Am. Chem. Soc.* **2012**, *134*, 3979−3982.
(4) Bunzli, J. C. G.; Piguet, C. *Chem. Soc. Rev.* **2005**, *34*, 1048−1077.
(5) Kreno, L. E.; Leong, K.; Farha, O. K.; Allendorf, M.; Van Duyne, R. P.; Hupp, J. T. *Chem. Rev.* **2012**, *112*, 1105−1125.
(6) Betard, A.; Fischer, R. A. *Chem. Rev.* **2012**, *112*, 1055−1083.
(7) Bradshaw, D.; Garai, A.; Huo, J. *Chem. Soc. Rev.* **2012**, *41*, 2344−2381.
(8) An, J.; Shade, C. M.; Chengelis-Czegan, D. A.; Petoud, S.; Rosi, N. L. *J. Am. Chem. Soc.* **2011**, *133*, 1220−1223.
(9) Luo, F.; Batten, S. R. *Dalton Trans.* **2010**, *39*, 4485−4488.
(10) Yu, J.; Cui, Y.; Wu, C.; Yang, Y.; Wang, Z.; O'Keeffe, M.; Chen, B.; Qian, G. *Angew. Chem., Int. Ed.* **2012**, *51*, 10542−10545.
(11) Esken, D.; Turner, S.; Wiktor, C.; Kalidindi, S. B.; Van Tendeloo, G.; Fischer, R. A. *J. Am. Chem. Soc.* **2011**, *133*, 16370−16373.
(12) Jin, S. Y.; Son, H. J.; Farha, O. K.; Wiederrecht, G. P.; Hupp, J. T. *J. Am. Chem. Soc.* **2013**, *135*, 955−958.
(13) Grusenmeyer, T. A.; Chen, J.; Jin, Y.; Nguyen, J.; Rack, J. J.; Schmehl, R. H. *J. Am. Chem. Soc.* **2012**, *134*, 7497−7506.
(14) Law, G.-L.; Pal, R.; Palsson, L. O.; Parker, D.; Wong, K.-L. *Chem. Commun.* **2009**, 7321−7323.
(15) Wang, Y. H.; Li, B.; Liu, Y. H.; Zhang, L. M.; Zuo, Q. H.; Shi, L. F.; Su, Z. M. *Chem. Commun.* **2009**, 5868−5870.
(16) Zhao, Q.; Li, F.; Huang, C. *Chem. Soc. Rev.* **2010**, *39*, 3007−3030.
(17) Xie, Z.; Ma, L.; deKrafft, K. E.; Jin, A.; Lin, W. *J. Am. Chem. Soc.* **2009**, *132*, 922−923.
(18) Ho, M.-L.; Chen, Y.-A.; Chen, T.-C.; Chang, P.-J.; Yu, Y.-P.; Cheng, K.-Y.; Shih, C.-H.; Lee, G.-H.; Sheu, H.-S. *Dalton Trans.* **2012**, *41*, 2592−2600.
(19) Barrett, S. M.; Wang, C.; Lin, W. *J. Mater. Chem.* **2012**, *22*, 10329−10334.
(20) Qi, X.; Liu, S.; Lin, R.; Liao, P.; Ye, J.; Lai, Z.; Guan, Y.; Cheng, X.; Zhang, J.; Chen, X. *Chem. Commun.* **2013**, *49*, 6864−6866.
(21) Lin, R.; Li, F.; Liu, S.; Qi, X.; Zhang, J.; Chen, X. *Angew. Chem., Int. Ed.* **2013**, *52*, 13429−13433.
(22) Parker, D.; Williams, J. A. G. *J. Chem. Soc., Dalton Trans.* **1996**, 3613−3628.
(23) Beeby, A.; Parker, D.; Williams, J. A. G. *J. Chem. Soc., Perkin Trans. 2* **1996**, 1565−1579.
(24) Zheng, S.-T.; Bu, J. T.; Li, Y.; Wu, T.; Zuo, F.; Feng, P.; Bu, X. *J. Am. Chem. Soc.* **2010**, *132*, 17062−17064.
(25) Zhang, F.; Zou, X.; Feng, W.; Zhao, X.; Jing, X.; Sun, F.; Ren, H.; Zhu, G. *J. Mater. Chem.* **2012**, *22*, 25019−25026.
(26) Souza, E. R.; Silva, I. G. N.; Teotonio, E. E. S.; Felinto, M. C. F. C.; Brito, H. F. *J. Lumin.* **2010**, *130*, 283−291.
(27) Dou, Z.; Yu, J.; Xu, H.; Cui, Y.; Yang, Y.; Qian, G. *Thin Solid Films* **2013**, *544*, 296.
(28) Volkringer, C.; Popov, D.; Loiseau, T.; Ferey, G.; Burghammer, M.; Riekel, C.; Haouas, M.; Taulclle, F. *Chem. Mater.* **2009**, *21*, 5695−5697.
(29) Haouas, M.; Volkringer, C.; Loiseau, T.; Ferey, G.; Tauelle, F. *J. Phys. Chem. C* **2011**, *115*, 17934−17944.
(30) Volkringer, C.; Leclerc, H.; Lavalley, J.-C.; Loiseau, T.; Ferey, G.; Daturi, M.; Vimont, A. *J. Phys. Chem. C* **2012**, *116*, 5710−5719.
(31) Dou, Z.; Yu, J.; Xu, H.; Cui, Y.; Yang, Y.; Qian, G. *Microporous Mesoporous Mater.* **2013**, *179*, 198−204.
(32) Yang, S.; Lin, X.; Blake, A. J.; Walker, G. S.; Hubberstey, P.; Champness, N. R.; Schroeder, M. *Nat. Chem.* **2009**, *1*, 487−493.
(33) Wu, W.; Rong, Y.; Zhao, B.; Sun, P.; Huang, X. *J. Lumin.* **2010**, *130*, 92−95.
(34) Dexter, D. L. *J. Chem. Phys.* **1953**, *21*, 836−850.
(35) Wang, Y.; Li, B.; Zhang, L.; Zuo, Q.; Li, P.; Zhang, J.; Su, Z. *ChemPhysChem* **2011**, *12*, 349−355.